AIAA JOURNAL
Vol. 32, No. 12, December 1994

Eigenanalysis of Unsteady Flows About Airfoils, Cascades, and Wings

Kenneth C. Hall*
Duke University, Durham, North Carolina 27708

A general technique for constructing reduced order models of unsteady aerodynamic flows about two-dimensional isolated airfoils, cascades of airfoils, and three-dimensional wings is developed. The starting point is a time domain computational model of the unsteady small disturbance flow. For illustration purposes, we apply the technique to an unsteady incompressible vortex lattice model. The eigenmodes of the system, which may be thought of as aerodynamic states, are computed and subsequently used to construct computationally efficient, reduced order models of the unsteady flowfield. Only a handful of the most dominant eigenmodes are retained in the reduced order model. The effect of the remaining eigenmodes is included approximately using a static correction technique. An important advantage of the present method is that once the eigenmode information has been computed, reduced order models can be constructed for any number of arbitrary modes of airfoil motion very inexpensively. Numerical examples are presented that demonstrate the accuracy and computational efficiency of the present method. Finally, we show how the reduced order model may be incorporated into an aeroelastic flutter model.

Introduction

In recent years, significant progress has been made in the development of unsteady aerodynamic analyses used to predict the flutter and forced response of isolated airfoils, cascades of airfoils, wings, and even complete aircraft configurations. Most unsteady aerodynamic models can be divided into two main groups: time domain analyses and frequency domain analyses.

In time domain analyses, one discretizes the governing equations on a computational mesh and then marches the solution from one time level to the next. At each time step, one imposes boundary conditions arising from either the prescribed motion of the airfoil or wing, or from a prescribed incident gust. For example, Davis and Bendiksen[1] have time marched the two-dimensional Euler equations to find the unsteady flow about vibrating airfoils. Batina[2] has computed the time dependent Euler flow about a complete harmonically deforming aircraft. Chaderjian and Guruswamy[3] have applied time marching techniques to solve the transonic Navier-Stokes equations about an oscillating wing. Time domain Euler and Navier-Stokes solvers have also been applied to unsteady flows in turbomachinery cascades, e.g., Refs. 4–8. The time domain analyses, although able to model extremely complex flow features and nonlinear effects, are computationally expensive due to the requirement that the solutions be both accurate and stable.

Using a frequency domain analysis (sometimes referred to as time linearized), one assumes that the unsteadiness is small compared to the mean flow. Thus, the unsteady flow is governed by linear small disturbance equations. The unsteady motion is assumed to be harmonic in time ($e^{i\omega t}$) so that the time derivative operator $\partial/\partial t$ gets replaced by $i\omega$. Hence, time does not appear explicitly in the governing equations. The resulting linear equations for the unsteady small disturbance flow can be solved very efficiently. The frequency domain approach has been applied to isolated airfoils,[9] two-dimensional cascades,[10–15] and three-dimensional cascades.[16]

One of the main difficulties with both the time domain and frequency domain techniques is that a separate analysis must be performed for each frequency and mode shape of interest. Unfortunately, in aeroelastic calculations, the frequency and mode shape are often not known a priori. A number of investigators have circumvented this difficulty by simultaneously marching the fluid dynamic and structural dynamic equations of motion (e.g., Refs. 17–19). This approach, although relatively straightforward, is still computationally very expensive. Furthermore, separate analyses must still be performed for each reduced velocity or mass ratio of interest. Additional analyses must also be performed if, for example, the aircraft configuration is modified by changing the configuration of under-wing stores. Finally, for applications to active control problems, such simulations do not provide the control engineer with the Laplace plane information needed to formulate control laws.

One approach to overcoming these difficulties is to develop "reduced order" models of the time domain or frequency domain aerodynamic analyses. The goal is to describe the unsteady aerodynamic loads over a range of reduced frequencies using models with a small number of aerodynamic states. One way to do this is to simply evaluate the unsteady load due to a particular mode shape of vibration at a number of reduced frequencies and then curve fit the results to a convenient time domain representation.[20–24] The approximate time domain representation is usually taken to be a sum of exponentials since the corresponding Laplace transform is a rational polynomial. The parameters in the approximation, such as the time constant of the exponentials or the constant multiplying each exponential, are found by minimizing the error between the approximation and the exact solution at a finite number of frequencies. Note that this method requires that approximations for the unsteady aerodynamic loads be computed for each mode shape of the vibrating wing or mode shape of gust disturbance. Also, this curve fitting approach provides little insight into the physics of the unsteady flowfield.

In structural dynamic problems, the dynamic behavior of complex structures is often reduced to a few degrees of freedom using normal mode analysis techniques. One might expect that some of these techniques could be applied to unsteady aerodynamic models. However, whereas modal analysis of structures is quite commonplace, modal analysis of unsteady aerodynamic systems is not. A notable early method to predict the natural modes of low-speed compressible flow about a cascade of unstaggered flat-plate airfoils was developed by Parker.[25] Parker found that the predicted eigenfrequencies of the system were in good agreement with experimentally observed acoustic resonances. More recently, Mahajan et al.[26] have computed the aeroelastic stability of a cascade of airfoils in compressible flow by computing the eigenvalues of the complete fluid/structure model. The airfoils were modeled using a typical section model; the flow was modeled using a two-dimensional time-marching potential code. In a recent paper by the author and

Received March 3, 1994; presented as Paper 94-1427 at the AIAA/ASME/ASCE/AHS/ASC Structures, Structural Dynamics and Materials Conference, Hilton Head, SC, April 18–20, 1994; revision received June 6, 1994; accepted for publication June 7, 1994.

*Assistant Professor, Department of Mechanical Engineering and Materials Science. Member AIAA.

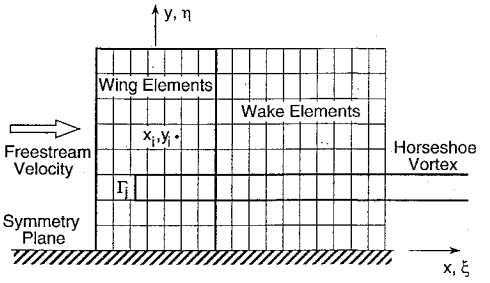

Fig. 1 Three-dimensional vortex lattice model of unsteady flow about a finite aspect ratio wing.

his colleagues,[27] the eigenvalues and eigenmodes of a frequency domain flow analysis of unsteady compressible flows about a cascade of airfoils were computed. The eigenmode information was then used to construct accurate, but very compact, reduced order aerodynamic models.

In this paper, the author describes how reduced order models may be constructed from time domain computational fluid dynamic (CFD) analyses. The method is general and may be applied to a wide variety of unsteady flow models. To demonstrate the approach, the method is applied here to a time domain vortex lattice model of unsteady incompressible flow. Numerical results are presented which show that only a few of the hundreds of eigenmodes of the system need to be retained in the reduced order aerodynamic model to obtain accurate results. Finally, the paper describes how the reduced order aerodynamic model may be incorporated into an aeroelastic model of flutter.

Theory

Vortex Lattice Model

The flow about a two-dimensional isolated airfoil, cascade of airfoils, or a three-dimensional wing is assumed to be incompressible, inviscid, and irrotational. Hence, the unsteady flowfield may be modeled using potential flow techniques. We use an unsteady vortex lattice method. A typical three-dimensional vortex lattice mesh used to compute the unsteady flow about a rectangular wing is shown in Fig. 1. For simplicity in the following description of the vortex lattice model, we limit the discussion to two-dimensional airfoils and cascades.

The airfoil and wake are divided into a number of elements. In the wake, the elements are all of equal size Δx in the streamwise direction. Point vortices are placed on the airfoil and in the wake at the quarter chord of the elements. At the three-quarter chord of each airfoil element is placed a collocation point. At these points, we require the velocity induced by the discrete vortices to equal the downwash arising from the unsteady motion of the airfoil. This relationship may be expressed as

$$w_i^{n+1} = \sum_{j=1}^{N} K_{ij}\Gamma_j^{n+1}, \qquad i = 1, \ldots, M \tag{1}$$

where w_i^{n+1} is the downwash at the ith collocation point at time level $n+1$, Γ_j is the strength of the jth vortex, and K_{ij} is a kernel function which depends on the particular problem being solved. Also, M is the number of vortex elements on the airfoil surface, and N is the total number of vortices on both the airfoil and wake. The downwash w_i^{n+1} may be the result of airfoil motion or, alternatively, due to an incident vortical gust.

For an isolated flat-plate airfoil in two-dimensional incompressible flow, the kernel function is given by

$$K_{ij} = 1/[2\pi(x_i - \xi_j)] \tag{2}$$

where x_i is the location of the ith collocation point, and ξ_j is the location of the jth vortex.

For a cascade of two-dimensional flat-plate airfoils, we consider the case in which the downwash on all of the airfoils is identical but shifted in phase by a constant interblade phase angle σ on each successive airfoil. Thus, the vortices on each airfoil and wake will be identical to the vortices on the reference airfoil and wake but shifted in phase by $r\sigma$ where r is the number of the airfoil in the cascade ($r = 0$ corresponds to the reference airfoil). Therefore, the kernel function represents the influence of an infinite row of phased vortices on the reference airfoil. An analytical form of this summation is given by Whitehead,[28]

$$K_{ij} = W(x_i - \xi_j) - W(-\infty) \tag{3}$$

where

$$W(z) = \frac{1}{4s}\left\{\frac{\exp[-(\pi-\sigma)\exp(i\Theta)z/s + i\Theta]}{\sinh[\pi\exp(i\Theta)z/s]} + \frac{\exp[+(\pi-\sigma)\exp(-i\Theta)z/s - i\Theta]}{\sinh[\pi\exp(-i\Theta)z/s]}\right\}$$

Here Θ is the stagger angle, s is the airfoil-to-airfoil gap, and the interblade phase angle σ is restricted to $0 \le \sigma < 2\pi$.

Next, we consider the modeling of the vorticity in the wake. Unsteady vorticity is shed in the wake; its strength is proportional to the time rate of change of circulation about the airfoil. If the time step Δt is taken to be equal to the time it takes the vorticity to convect from one vortex station to the next ($\Delta t = U\Delta x$), then the strength of the first vortex point in the wake at the time level $n+1$ is given by

$$\Gamma_{M+1}^{n+1} = -\sum_{j=1}^{M}\left(\Gamma_j^{n+1} - \Gamma_j^n\right) \tag{4}$$

Once the vorticity has been shed into the wake, it is convected in the wake with speed U, the freestream velocity. For the special case where $\Delta t = U\Delta x$, this convection is described numerically by

$$\Gamma_i^{n+1} = \Gamma_{i-1}^n, \qquad i = M+2, N-1 \tag{5}$$

Finally, because the vortex sheet is infinitely long but the computational model has a finite length wake, special treatment is required at the last vortex element. Otherwise, the starting vortex would disappear abruptly when it reaches the end of the computational wake producing a discontinuous change in the induced wash at the airfoil. To alleviate this difficulty, the convected vorticity, upon reaching the end of the wake, is allowed to dissipate smoothly using the following relationship:

$$\Gamma_i^{n+1} = \Gamma_{i-1}^n + \alpha\Gamma_i^n, \qquad i = N \tag{6}$$

where α is a relaxation factor. For the isolated airfoil problem, the relaxation factor is selected so that the unsteady indicial response agrees well with the Wagner indicial response function[29]; usually, $0.95 < \alpha < 1.0$.

Putting together the kernel function equations [Eq. (1) and Eq. (2) or Eq. (3)], the conservation of circulation [Eq. (4)], and the wake convection equations [Eqs. (5) and (6)] gives in matrix notation

$$\mathbf{A}\boldsymbol{\Gamma}^{n+1} + \mathbf{B}\boldsymbol{\Gamma}^n = \mathbf{w}^{n+1} \tag{7}$$

where $\boldsymbol{\Gamma}$ is a vector containing the strengths of the vortex elements and $\mathbf{w}$ is the vector containing the prescribed downwash. The matrices $\mathbf{A}$ and $\mathbf{B}$ are large sparse matrices.

Given a prescribed time history of the downwash, Eq. (7) is simply marched in time from one time level to the next to find the time history of the strengths of the vortex elements. Conceptually, the solution at time level $n+1$ is expressed in terms of the solution at time level n by

$$\boldsymbol{\Gamma}^{n+1} = \mathbf{A}^{-1}[\mathbf{w}^{n+1} - \mathbf{B}\boldsymbol{\Gamma}^n] \tag{8}$$

Of course, the matrix $\mathbf{A}$ is not actually inverted. Instead, the matrix $\mathbf{A}$ is decomposed just once using lower-upper (LU) decomposition. Then, at each time step, Eq. (8) is solved using one forward and one back substitution.

Once the time history of the unsteady vorticity has been computed, one can compute the unsteady lift and moment acting on the

airfoil. Making use of Bernoulli's equation, one finds that the unsteady lift L and moment M_{EA} measured about the elastic axis are given by

$$L = \int_{-b}^{b} \rho \left[U\gamma(x) + \frac{\mathrm{d}}{\mathrm{d}t} \int_{-b}^{x} \gamma(x_1)\mathrm{d}x_1 \right] \mathrm{d}x \tag{9}$$

$$M_{EA} = \int_{-b}^{b} \rho(x-e) \left[U\gamma(x) + \frac{\mathrm{d}}{\mathrm{d}t} \int_{-b}^{x} \gamma(x_1)\mathrm{d}x_1 \right] \mathrm{d}x \tag{10}$$

where γ is the (continuous) vorticity on the airfoil surface, ρ the density, b the semichord of the airfoil, and e the distance of the elastic axis aft of the midchord. Discretizing Eqs. (9) and (10) gives

$$L^{n+\frac{1}{2}} = \mathbf{I}_1 \cdot \mathbf{\Gamma}^n + \mathbf{I}_2 \cdot \mathbf{\Gamma}^{n+1} \tag{11}$$

$$M_{EA}^{n+\frac{1}{2}} = \mathbf{I}_3 \cdot \mathbf{\Gamma}^n + \mathbf{I}_4 \cdot \mathbf{\Gamma}^{n+1} \tag{12}$$

where $\mathbf{I}_1$, $\mathbf{I}_2$, $\mathbf{I}_3$, and $\mathbf{I}_4$ are row vectors which approximate the integral operators in Eqs. (9) and (10).

Finally, although the preceding development is for two-dimensional flows, we have implemented a similar unsteady vortex lattice method for flows about three-dimensional wings.

Reduced Order Aerodynamic Model

In this section, we derive a reduced order model of the vortex lattice model described earlier. Consider the generalized eigenvalue problem

$$z_i \mathbf{A}\mathbf{x}_i + \mathbf{B}\mathbf{x}_i = \mathbf{0} \tag{13}$$

where z_i is the ith eigenvalue and $\mathbf{x}_i$ is the corresponding right eigenvector, and the matrices $\mathbf{A}$ and $\mathbf{B}$ are the same as those given in Eq. (7). More generally, we may write

$$\mathbf{AXZ} + \mathbf{BX} = \mathbf{0} \tag{14}$$

where $\mathbf{Z}$ is a diagonal matrix containing the eigenvalues of the generalized eigenvalue problem, and $\mathbf{X}$ is a matrix whose columns contain the corresponding right eigenvectors. Similarly, the left eigenvector problem is given by

$$\mathbf{A}^T\mathbf{YZ} + \mathbf{B}^T\mathbf{Y} = \mathbf{0} \tag{15}$$

The eigenvectors satisfy the orthogonality conditions

$$\mathbf{Y}^T\mathbf{AX} = \mathbf{I} \tag{16}$$

$$\mathbf{Y}^T\mathbf{BX} = -\mathbf{Z} \tag{17}$$

The eigenvalues and eigenvectors describe the natural modes of fluid motion or, at least, the natural modes of the computational model of fluid motion. If the magnitude of all of the eigenvalues is less than or equal to unity, as is usually the case, then the system is stable. If any of the eigenvalues is greater than unity, then the system is unstable. The discrete time eigenvalues z_i are related to the more familiar continuous time eigenvalues λ_i by $z_i = \exp(\lambda_i \Delta t)$.

For the relatively small problems considered in this paper ($N < 500$), we compute all of the eigenmodes using the well-known Eispack routines.[30] For larger problems, one would compute only a small subset of the eigenmodes using algorithms that take advantage of the sparseness of the system of equations. For convenience, we reorder the modes according to the magnitude of the eigenvalue z_i from largest to smallest.

Next, as is commonly done in structural dynamic problems, we reduce the order of the flow model using the "mode superposition method." We represent the dynamic behavior of the fluid as the sum of individual eigenmodes, i.e.,

$$\mathbf{\Gamma} = \mathbf{Xc} \tag{18}$$

where $\mathbf{c}$ is the vector of normal mode coordinates. Substitution of Eq. (18) into Eq. (7) gives

$$\mathbf{AXc}^{n+1} + \mathbf{BXc}^n = \mathbf{w}^{n+1} \tag{19}$$

Next, premultiplying Eq. (19) by $\mathbf{Y}^T$ and making use of the orthogonality conditions gives a set of N uncoupled equations for the modal coordinates $\mathbf{c}$,

$$\mathbf{c}^{n+1} - \mathbf{Zc}^n = \mathbf{Y}^T\mathbf{w}^{n+1} \tag{20}$$

Because the left-hand side of Eq. (20) is now diagonal, each mode can be marched forward in time independently and inexpensively. The results can then be reassembled using Eq. (18) to obtain the strength of the vortex elements.

The advantage to a modal approach is that one may construct a reduced order model by retaining only a few of the original modes. For the present analysis, we retain the m modes with the largest eigenvalues z_i (i.e., the most lightly damped eigenmodes) where $m \ll N$. Therefore, in Eqs. (18) and (20), $\mathbf{X}$ and $\mathbf{Y}$ are reduced to $N \times m$ matrices, and $\mathbf{Z}$ is reduced to an $m \times m$ matrix.

Unfortunately, one finds that in some cases the reduced order model does not produce satisfactory results unless a prohibitively large number of modes are used. The problem occurs because the neglected modes are not orthogonal to the downwash and, therefore, participate in the response. However, since the neglected modes tend to have large natural frequencies compared to the excitation frequency, the neglected eigenmodes respond in an essentially quasistatic fashion. Hence, to include approximately the effects of the neglected eigenmodes, we decompose the unsteady solution into two parts, a part which is equivalent to the response the system would have if the disturbance were quasisteady and a dynamic part to be determined, i.e.,

$$\begin{aligned} \mathbf{\Gamma}^n &= \mathbf{\Gamma}_s^n + \tilde{\mathbf{\Gamma}}^n \\ &= \mathbf{\Gamma}_s^n + \mathbf{X}\tilde{\mathbf{c}}^n \end{aligned} \tag{21}$$

The quasisteady portion $\mathbf{\Gamma}_s$ is given by

$$[\mathbf{A} + \mathbf{B}]\mathbf{\Gamma}_s^n = \mathbf{w}^n \tag{22}$$

Thus, Eq. (20) is replaced by

$$\tilde{\mathbf{c}}^{n+1} - \mathbf{Z}\tilde{\mathbf{c}}^n = \mathbf{Y}^T\mathbf{w}^{n+1} - \mathbf{Y}^T\left(\mathbf{A}\mathbf{\Gamma}_s^{n+1} + \mathbf{B}\mathbf{\Gamma}_s^n\right) \tag{23}$$

The static portion of the solution, described by Eq. (22), includes the influence of all of the eigenmodes. For the dynamic part of the solution, described by Eq. (23), only a small number of modes need to be retained since only the low-frequency modes respond in a dynamic way.

This approach is the discrete time analog of the static correction or mode acceleration methods commonly used in structural dynamics.[31] The advantage of Eq. (23) over Eq. (20) is that generally many fewer modes must be retained to obtain an accurate solution. The additional cost of the LU decomposition required in Eq. (22) is small compared to the cost of computing the larger number of eigenmodes that would be required to obtain accurate solutions using the mode superposition method without the static correction.

Aeroelastic Model

Having described the reduced order modeling technique, we now briefly describe how one would incorporate the reduced order aerodynamic model into an aeroelastic model of flutter. Consider a structural dynamic model of an airfoil or wing. The governing equations of motion, when cast in discrete time form, will take the form

$$\mathbf{D}_2\mathbf{q}^{n+1} + \mathbf{D}_1\mathbf{q}^n + \mathbf{f}^{n+\frac{1}{2}} = \mathbf{0} \tag{24}$$

where vector $\mathbf{q}$ is the state of the airfoil, and $\mathbf{D}_1$ and $\mathbf{D}_2$ are matrices describing the structural dynamic behavior of the airfoil typical section or wing. The unsteady aerodynamic loads appear in the vector $\mathbf{f}$, and may be expressed in terms of the unsteady vortex elements as

$$\mathbf{f}^{n+\frac{1}{2}} = \mathbf{C}_2\mathbf{\Gamma}^{n+1} + \mathbf{C}_1\mathbf{\Gamma}^n \tag{25}$$

Note that the matrices $\mathbf{C}_1$ and $\mathbf{C}_2$ are quite sparse since only the vortex elements on the airfoil itself contribute directly to the aerodynamic loads.

Similarly, the downwash w on the airfoil is due to two sources: incident vortical gusts and motion of the airfoil itself, i.e.,

$$\mathbf{w} = \mathbf{w}_g + \mathbf{Eq} \tag{26}$$

where $\mathbf{E}$ is a matrix describing the linear relationship between the motion of the airfoil and the resulting downwash at the collocation points.

Putting Eq. (7) and Eqs. (24–26) together in matrix form gives

$$\begin{bmatrix} \mathbf{A} & \mathbf{E} \\ \mathbf{C}_2 & \mathbf{D}_2 \end{bmatrix} \begin{Bmatrix} \boldsymbol{\Gamma} \\ \mathbf{q} \end{Bmatrix}^{n+1} + \begin{bmatrix} \mathbf{B} & \mathbf{0} \\ \mathbf{C}_1 & \mathbf{D}_1 \end{bmatrix} \begin{Bmatrix} \boldsymbol{\Gamma} \\ \mathbf{q} \end{Bmatrix}^{n} = \begin{Bmatrix} \mathbf{w}_g \\ \mathbf{0} \end{Bmatrix}^{n+1} \tag{27}$$

We refer to Eq. (27) as the complete fluid/structure model. The eigenvalues of the homogeneous part of Eq. (27) determine the stability of the aeroelastic system. If any of the eigenvalues z_i have magnitude greater than unity, then the system is unstable.

In principle, one could find the eigenvalues of Eq. (27) directly. However, for most aeroelastic calculations, one must compute the eigenvalues of the system as some parameter—such as the reduced velocity—varies. Under these circumstances, it is computationally much more efficient to model the unsteady aerodynamic loads using the reduced order aerodynamic model presented in the previous section. Changing to normal mode coordinates [see Eq. (18)] and premultiplying the upper portion of Eq. (27) by $\mathbf{Y}^T$ gives

$$\begin{bmatrix} \mathbf{I} & \mathbf{Y}^T\mathbf{E} \\ \mathbf{C}_2\mathbf{X} & \mathbf{D}_2 \end{bmatrix} \begin{Bmatrix} \mathbf{c} \\ \mathbf{q} \end{Bmatrix}^{n+1} + \begin{bmatrix} -\mathbf{Z} & \mathbf{0} \\ \mathbf{C}_1\mathbf{X} & \mathbf{D}_1 \end{bmatrix} \begin{Bmatrix} \mathbf{c} \\ \mathbf{q} \end{Bmatrix}^{n} = \begin{bmatrix} \mathbf{Y}^T \\ \mathbf{0} \end{bmatrix} \{\mathbf{w}_g\}^{n+1} \tag{28}$$

Finally, incorporating the static correction technique into the reduced order aerodynamic model, and after some manipulation, one obtains

$$\begin{bmatrix} \mathbf{I} & \mathbf{Y}^T[\mathbf{I} + \mathbf{A}(\mathbf{A}+\mathbf{B})^{-1}]\mathbf{E} \\ \mathbf{C}_2\mathbf{X} & \mathbf{D}_2 + \mathbf{C}_2(\mathbf{A}+\mathbf{B})^{-1}\mathbf{E} \end{bmatrix} \begin{Bmatrix} \tilde{\mathbf{c}} \\ \mathbf{q} \end{Bmatrix}^{n+1} + \begin{bmatrix} -\mathbf{Z} & \mathbf{Y}^T\mathbf{B}(\mathbf{A}+\mathbf{B})^{-1}\mathbf{E} \\ \mathbf{C}_1\mathbf{X} & \mathbf{D}_1 + \mathbf{C}_1(\mathbf{A}+\mathbf{B})^{-1}\mathbf{E} \end{bmatrix} \begin{Bmatrix} \tilde{\mathbf{c}} \\ \mathbf{q} \end{Bmatrix}^{n} = \begin{bmatrix} \mathbf{Y}^T[\mathbf{I} - \mathbf{A}(\mathbf{A}+\mathbf{B})^{-1}] \\ -\mathbf{C}_2(\mathbf{A}+\mathbf{B})^{-1} \end{bmatrix} \{\mathbf{w}_g\}^{n+1} + \begin{bmatrix} \mathbf{Y}^T[\mathbf{I} - \mathbf{B}(\mathbf{A}+\mathbf{B})^{-1}] \\ -\mathbf{C}_1(\mathbf{A}+\mathbf{B})^{-1} \end{bmatrix} \{\mathbf{w}_g\}^{n} \tag{29}$$

The eigenvalues of Eq. (29) will closely approximate the eigenvalues of Eq. (27) provided that a sufficient number of eigenmodes are retained in the model.

Numerical Results

Vortex Lattice Model

The results in this section are presented to validate the unsteady vortex lattice model. Consider the lift acting on an isolated flat-plate airfoil due to a step change in airfoil downwash (the Wagner problem). Shown in Fig. 2 is the step response computed using the present vortex lattice method. The airfoil was modeled using 20 vortex elements. The wake was modeled using 200 vortex elements, the length of the wake was taken to be 10 chord lengths, and the vortex relaxation factor α was taken to be 0.996. Also shown in Fig. 2 for comparison is the Wagner function.[29] The present theory is seen to be in almost perfect agreement with the Wagner function.

Also shown in Fig. 2 is the computed indicial response for a cascade of two-dimensional flat-plate airfoils. The cascade has a stagger angle Θ of 45 deg, and a gap-to-chord ratio G of 1.0. For the case considered here, the interblade phase angle σ is 180 deg. The airfoil was modeled using 20 vortex elements. The wake length was taken to be five chord lengths and was modeled using 100 vortex elements. The vortex relaxation factor α was set to 0.5. The cascade indicial response is seen to be somewhat larger than the airfoil indicial response. Furthermore, the lift is seen to rise to its

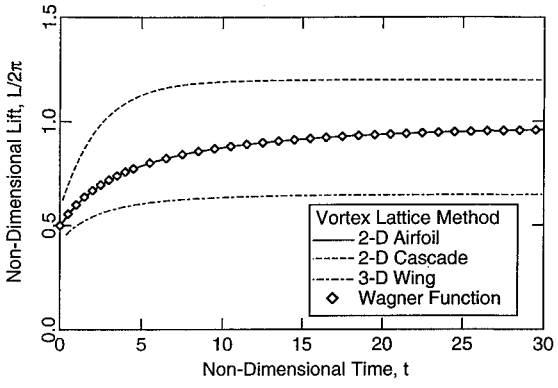

Fig. 2 Time history of unsteady lift due to step change in downwash for two-dimensional isolated airfoil, cascade of two-dimensional airfoils, and three-dimensional wing.

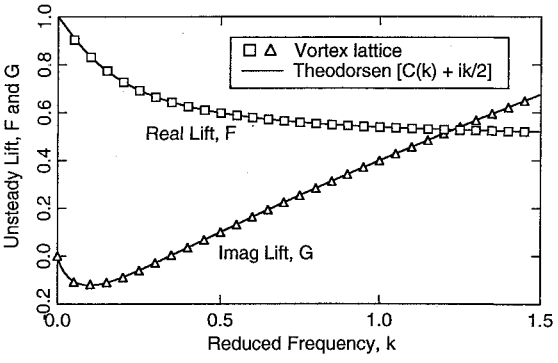

Fig. 3 Unsteady lift due to harmonic plunging motion of a two-dimensional airfoil.

asymptotic value faster than in the isolated airfoil case. The reason for difference in the rise times can be found by examining the kernel functions for these two cases. For the case of the airfoil, the influence of vorticity varies like the inverse of the distance from the airfoil. Thus, asymptotically, the lift approaches its final value like $1/t$. In the cascade case, however, the influence of the vorticity decays exponentially for large t (for nonzero interblade phase angles). This is because the shed vorticity from each of the blades of the cascade is equal in magnitude but shifted in phase by integer multiples of the interblade phase angle. The influence of the far wake is reduced by destructive interference. The result is that only a finite portion of the near wake has any influence on the cascade.

Finally, Fig. 2 shows the indicial response of a rectangular wing with an aspect ratio of 5.0 due to rigid-body plunging motion of the wing. To reduce the number of vortex elements required, the solution was assumed to be symmetric about the longitudinal axis. For this example, the wing was modeled with eight vortex elements in the streamwise direction, and 10 in the spanwise direction. The wake was taken to be five chords long and was modeled using 40 vortex elements in the streamwise direction and 10 in the spanwise direction. The wake relaxation factor α was set to 0.992. Note that the asymptotic value of the nondimensional lift (0.65) is somewhat less than that of the two-dimensional isolated airfoil (1.0). This is to be expected because of the reduction of the steady lift curve slope with decreasing finite aspect ratio (for an elliptic wing, the asymptotic value would be 0.714). Also, the rise time is somewhat shorter than in the case of the isolated airfoil. This is because the influence of a convected horseshoe vortex varies like $1/t^2$ for large t rather than $1/t$ as in the case of a two-dimensional vortex.

Next, to demonstrate the frequency domain analysis capabilities of the vortex lattice model, the unsteady lift due to plunging motion of an isolated airfoil was computed for a range of reduced frequencies. The results are plotted in Fig. 3. Also shown for comparison is the exact solution to the isolated airfoil problem due to Theodorsen.[32] Note that because the vortex lattice model does not separately compute circulatory and noncirculatory lift, the apparent

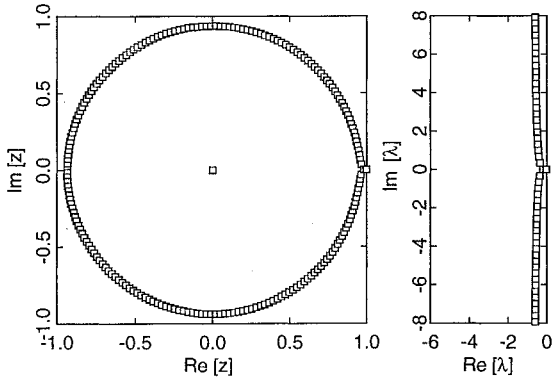

Fig. 4 Eigenvalues of vortex lattice model of unsteady flow about a two-dimensional isolated airfoil.

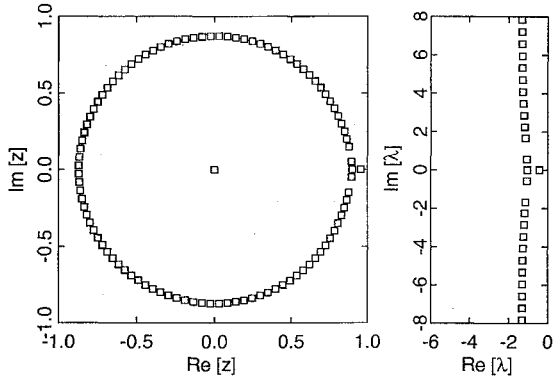

Fig. 5 Eigenvalues of vortex lattice model of unsteady flow about a cascade of two-dimensional airfoils.

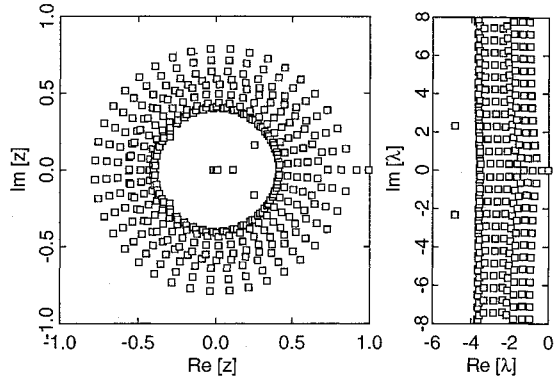

Fig. 6 Eigenvalues of vortex lattice model of unsteady flow about a three-dimensional wing, aspect ratio = 5.0; only symmetric modes shown.

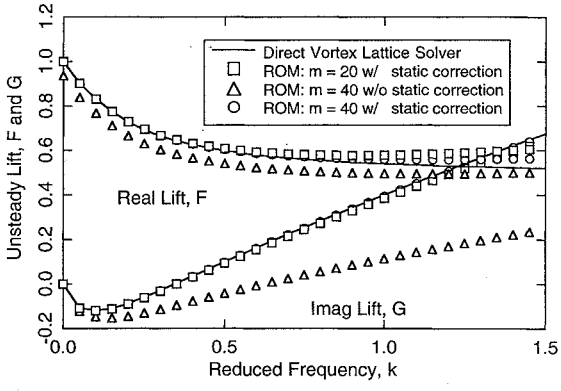

Fig. 7 Unsteady lift predicted using reduced order modeling technique for the case of a harmonically plunging isolated airfoil.

mass effects have been added to Theodorsen's circulatory lift function. The results are seen to been quite satisfactory for the range of reduced frequencies considered here.

Eigenmodes of Aerodynamic Systems

Next, having validated the vortex lattice model, the eigenmodes and eigenvalues of the three aerodynamic systems described earlier were computed. A typical computational result is shown in Fig. 4. Shown are the eigenvalues for the isolated airfoil case in both z-plane and λ-plane interpretations. Note that the eigenvalues are lightly damped and form a dense line which runs close to the imaginary axis in the λ plane. The line of eigenvalues intersects the real axis very near the origin and may be thought of as approximating a branch cut of the aerodynamic transfer function. Numerical experiments reveal that this line of eigenvalues gets denser as the length of the computational wake is increased with constant element size Δx. The line of eigenvalues gets longer as the element size Δx is reduced with constant wake length.

The presence of a branch cut is consistent with the well-known result that the Theodorsen function contains a branch point at the origin. However, the branch cut is usually taken to be along the negative real axis. For example, Desmarais[33] found a continued fraction representation of the Theodorsen function. The poles (eigenvalues) of this continued fraction form a dense line along the negative real axis. Also, a number of investigators[20–24] have developed curve fits to the Theodorsen function and have explicitly placed the poles on the negative real axis. The reason that the eigenvalues of the present vortex lattice model appear in lightly damped complex conjugate pairs rather than as real negative eigenvalues is not completely understood; but neither is the present method thought to be erroneous. Instead, the present analysis gives an equally valid approximation to the aerodynamic transfer function.

Shown in Fig. 5 are the eigenvalues for the cascade of flat plates previously considered. Again, there is a line of closely spaced eigenvalues (a branch cut). In this case, however, the branch cut is shifted to the left in the complex plane. Note also the simple pole between the branch cut and the origin. Because the poles are shifted to the left, the eigenmodes will decay more quickly than in the case of the isolated airfoil. Thus, for the indicial response problem, the final lift will be reached more quickly. This is clearly seen to be the case in Fig. 2.

Finally, shown in Fig. 6 are the eigenvalues of the vortex lattice model of unsteady flow about a rectangular wing with an aspect ratio of 5.0. Since symmetry about the longitudinal axis was used to reduce the number of degrees of freedom in the vortex lattice model, only the eigenvalues corresponding to symmetric eigenmodes are shown. Note that in the λ plane, the eigenvalues appear to form a number of branch cuts, each successive branch cut shifted to the left. Careful inspection reveals that there are 10 branch cuts, the same number as the number of vortex elements in the spanwise direction. The branch farthest to the right corresponds to the first spanwise mode, that is, the mode in which the vortex elements vary most slowly in the spanwise direction (much like the first vibrational mode of a beam).

Reduced Order Aerodynamic Models

Next, we use the eigenmode information computed in the previous section to construct reduced order aerodynamic models. Figure 7 shows the unsteady lift predicted using the reduced order modeling technique for the case of a harmonically plunging isolated airfoil. Three cases are considered. In two cases, 20 or 40 of the most lightly damped eigenmodes are retained, and a static correction is used to approximate the influence of the remaining eigenmodes. In the third case, 40 eigenmodes are retained, but no static correction is performed. Also shown in Fig. 7 is the direct vortex lattice solution. Both the reduced order models using the static correction give quite good predictions up to a reduced frequency of 1.5, although the 40-mode model is slightly more accurate. The reduced order model without the static correction, on the other hand, gives poor results. The real part of the unsteady lift has an almost constant error. The error in the imaginary part is zero at a reduced frequency of zero, but grows quite large as the reduced frequency increases.

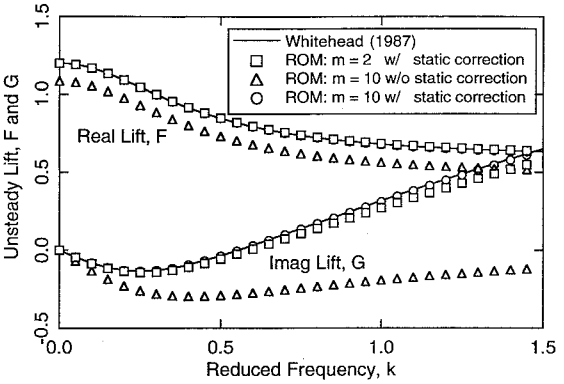

Fig. 8 Unsteady lift due to harmonic plunging motion of a cascade of two-dimensional airfoils predicted using reduced order models.

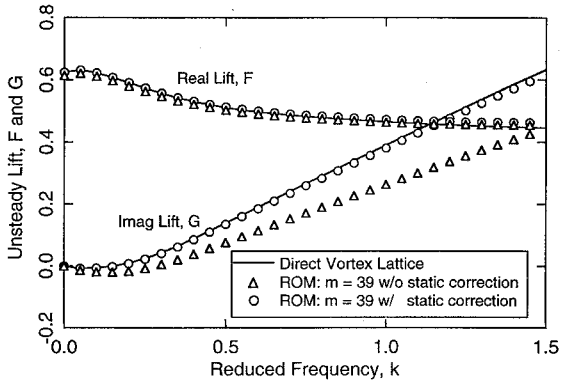

Fig. 9 Unsteady lift due to harmonic rigid body plunging motion of a three-dimensional wing, aspect ratio = 5.

Figure 8 shows a typical reduced order model calculation for a cascade of airfoils. For the case shown here, the airfoils vibrate in plunge with interblade phase angle σ of 180 deg. The reduced order model was constructed using two or 10 eigenmodes together with a static correction, and 10 modes without a static correction. Also shown is the semianalytical solution due to Whitehead.[28] The 10-mode solution using the static correction agrees almost exactly with Whitehead's solution. Even the two-mode solution agrees quite well. This demonstrates that the dynamic behavior of the unsteady flow in cascades is governed by just a few important eigenmodes. Hall et al.[27] found similar results for compressible flow through cascades.

Finally, we consider the case of the finite wing vibrating with a rigid-body plunging motion. Two reduced order models were used: both contained 39 eigenmodes, but one used the static correction technique and one did not. Figure 9 shows the unsteady lift as a function of reduced frequency. The results are similar to those found for the two-dimensional isolated airfoil and cascade examples, that is, the reduced order model using the static correction agrees well with the direct vortex lattice solver, whereas the reduced order model without the static correction has significant errors at high reduced frequencies.

One interesting feature of the case shown in Fig. 9 is that most of the eigenmodes used in the reduced order model were eigenmodes of the first mode branch cut (the branch cut nearest the imaginary axis). This suggests that one might be able to reduce the size of the vortex lattice model by using vorticity distributed in a few appropriately shaped spanwise modes.

Another interesting point is that no more modes were required to obtain satisfactory results for a finite wing than were required for the two-dimensional airfoil, even though the wing has a total of 480 degrees of freedom in the model compared to 220 in the case of the two-dimensional airfoil (in fact, the finite wing results are slightly more accurate). This is an important result. The author believes that similar results will hold when the reduced order modeling technique is applied to large three-dimensional CFD algorithms. That is, only a very few of the thousands of eigenmodes will contribute dynamically to the unsteady flow solution (although a static correction will generally be needed to approximate the influence of the eigenmodes not included).

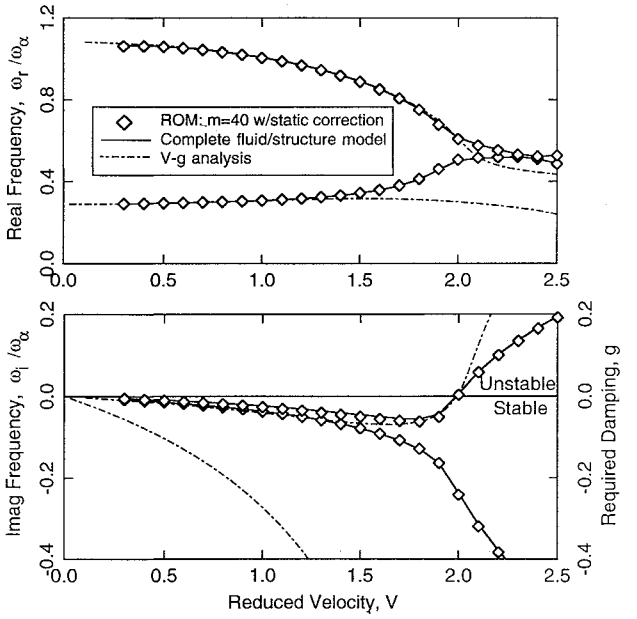

Fig. 10 Natural frequencies and damping of the aeroelastic modes of a typical section model.

Flutter Calculations

Next, we consider the use of reduced order models to compute the flutter stability of a two-dimensional airfoil. The typical section model has two degrees of freedom, one plunging and one pitching. The mass ratio μ is 20, the static imbalance x_α/b is 0.2, the radius of gyration r_α/b is 0.5, and the location of elastic axis aft of midchord e/b is -0.1 (i.e., it is in front of the midchord). Finally, the frequency ratio ω_h/ω_α of the uncoupled modes is 0.3, where ω_h and ω_α are the uncoupled plunging and torsional frequencies, respectively. Shown in Fig. 10 are the real and imaginary parts of the frequencies of the aeroelastic modes ($\lambda = i\omega_r - \omega_i$). These results were computed using the complete vortex lattice model coupled directly to the structural dynamic model [Eq. (27)] and using the reduced order aerodynamic model coupled to the structural dynamic model [Eq. (29)]. Here, 40 eigenmodes were used in the reduced order model along with a static correction. The frequencies and damping of the aeroelastic modes calculated using the complete and reduced order models are seen to be very good agreement. Note that flutter occurs at a reduced velocity V of 2.0 where $V = U/(\omega_\alpha b)$ and is of the frequency coalescence type. Also shown for comparison is a classical *V-g* calculation using Theodorsen aerodynamics. The flutter speed predicted using the *V-g* method is nearly identical to that predicted using the present method. However, the frequencies and "required damping" g predicted using the *V-g* method are not physically meaningful except at the flutter speed, and then only for the mode which is neutrally stable.

Of course, the reduced order model required much less computational time to solve than the complete model. For the case considered here, the reduced order modeling approach required that a single generalized eigenvalue problem with 220 degrees of freedom be solved just once. Then, for each reduced velocity, an eigenvalue problem with 44 degrees of freedom was solved (40 reduced aerodynamic states plus four structural dynamic states). The complete fluid/structure problem, on the other hand, required that an eigenvalue problem with 224 degrees of freedom be solved at every reduced frequency. Since the computational time required to solve an eigenvalue problem increases rapidly with the size of the problem, the computational savings afforded by the present method are substantial. For example, to compute the aeroelastic stability using

the reduced order model required a single calculation taking about 16 s on a Silicon Graphics Indigo 4400 workstation to form the reduced order aerodynamic model. Then, for each reduced frequency, the aeroelastic stability calculation required approximately 0.4 s. This compares to about 14 s per reduced frequency for the complete fluid/structure model.

Conclusions

A novel reduced order modeling technique has been applied to unsteady fluid motions about two-dimensional isolated airfoils, cascades of airfoils, and three-dimensional wings. It was shown that the unsteady fluid motion can be modeled accurately using just a small number of aerodynamic eigenmodes provided a static correction is applied to approximate the influence of the remaining eigenmodes. Such a reduced order model is particularly useful when a large number of aeroelastic calculations are to be performed. The form of the reduced order model, a low-order model with a classical pole/zero behavior of the aerodynamic transfer function, should also prove useful in applications of active control of aeroelastic phenomena. Furthermore, the reduced order model provides important insights about the nature of unsteady flows about airfoils, cascades, and wings. Finally, although the method was applied to a relatively simple flow model in this paper, the reduced order modeling technique can be applied to more sophisticated computational fluid dynamic models of unsteady compressible flow.[27]

Acknowledgments

The author would like to thank Earl Dowell, Dean of the School of Engineering at Duke University, and Răzvan Florea and Michael Romanowski, Research Assistants in the Department of Mechanical Engineering and Materials Science at Duke University, for their helpful comments on reduced order modeling.

References

[1]Davis, G. A., and Bendiksen, O. O., "Unsteady Transonic Two-Dimensional Euler Solutions Using Finite Elements," *AIAA Journal*, Vol. 31, No. 6, 1993, pp. 1051–1059.

[2]Batina, J. T., "Unsteady Euler Algorithm with Unstructured Dynamic Mesh for Complex-Aircraft Aerodynamic Analysis," *AIAA Journal*, Vol. 29, No. 3, 1991, pp. 327–333.

[3]Chaderjian, N. M., and Guruswamy, G. P., "Transonic Navier-Stokes Computations for an Oscillating Wing Using Zonal Grids," *Journal of Aircraft*, Vol. 29, No. 3, 1992, pp. 326–335.

[4]Giles, M. B., "Calculation of Unsteady Wake/Rotor Interaction," *Journal of Propulsion and Power*, Vol. 4, No. 4, 1988, pp. 356–362.

[5]Gerolymos, G. A., "Advances in the Numerical Integration of the Three-Dimensional Euler Equations in Vibrating Cascades," *Journal of Turbomachinery*, Vol. 115, No. 4, 1993, pp. 781–790.

[6]Huff, D. L., Swafford, T. W., and Reddy, T. S. R., "Euler Flow Predictions for an Oscillating Cascade Using a High Resolution Wave-Split Scheme," American Society of Mechanical Engineers, ASME Paper 91-GT-198, June 1991.

[7]Rai, M. M., "Three-Dimensional Navier-Stokes Simulations of Turbine Rotor Stator Interaction, Part I—Methodology," *Journal of Propulsion and Power*, Vol. 5, No. 3, 1989, pp. 307–311.

[8]Rai, M. M., "Three-Dimensional Navier-Stokes Simulations of Turbine Rotor Stator Interaction, Part II—Results," *Journal of Propulsion and Power*, Vol. 5, No. 3, 1989, pp. 312–319.

[9]Ehlers, F. E., and Weatherill, W. H., "A Harmonic Analysis Method for Unsteady Transonic Flow and Its Application to the Flutter of Airfoils," NASA CR-3537, May 1982.

[10]Verdon, J. M., and Caspar, J. R., "A Linearized Unsteady Aerodynamic Analysis for Transonic Cascades," *Journal of Fluid Mechanics*, Vol. 149, Dec. 1984, pp. 403–429.

[11]Whitehead, D. S., and Grant, R. J., "Force and Moment Coefficients of High Deflection Cascades," *Proceedings of the 2nd International Symposium on Aeroelasticity in Turbomachines*, edited by P. Suter, Juris-Verlag, Zurich, Switzerland, 1981, pp. 85–127.

[12]Hall, K. C., "Deforming Grid Variational Principle for Unsteady Small Disturbance Flows in Cascades," *AIAA Journal*, Vol. 31, No. 5, 1993, pp. 891–900.

[13]Hall, K. C., and Crawley, E. F., "Calculation of Unsteady Flows in Turbomachinery Using the Linearized Euler Equations," *AIAA Journal*, Vol. 27, No. 6, 1989, pp. 777–787.

[14]Holmes, D. G., and Chuang, H. A., "2D Linearized Harmonic Euler Flow Analysis for Flutter and Forced Response," *Unsteady Aerodynamics, Aeroacoustics, and Aeroelasticity of Turbomachines and Propellers*, edited by H. M. Atassi, Springer-Verlag, New York, 1993, pp. 213–230.

[15]Hall, K. C., and Clark, W. S., "Linearized Euler Prediction of Unsteady Aerodynamic Loads in Cascades," *AIAA Journal*, Vol. 31, No. 3, 1993, pp. 540–550.

[16]Hall, K. C., and Lorence, C. B., "Calculation of Three-Dimensional Unsteady Flows in Turbomachinery Using the Linearized Harmonic Euler Equations," *Journal of Turbomachinery*, Vol. 115, No. 4, 1993, pp. 800–809.

[17]Rausch, R. D., Batina, J. T., and Yang, T. Y., "Three-Dimensional Time-Marching Aeroelastic Analyses Using an Unstructured-Grid Euler Method," *AIAA Journal*, Vol. 31, No. 9, 1993, pp. 1626–1633.

[18]Robinson, B. A., Batina, J. T., and Yang, T. Y., "Aeroelastic Analysis of Wings Using the Euler Equations with a Deforming Mesh," *Journal of Aircraft*, Vol. 28, No. 11, 1991, pp. 781–788.

[19]Bendiksen, O. O., and Kousen, K. A., "Transonic Flutter Analysis Using the Euler Equations," AIAA Paper 87-0911, April 1987.

[20]Dowell, E. H., "A Simple Method for Converting Frequency Domain Aerodynamics to the Time Domain," NASA TM-81844, Oct. 1980.

[21]Peterson, L. D., and Crawley, E. F., "Improved Exponential Time Series Approximation of Unsteady Aerodynamic Operators," *Journal of Aircraft*, Vol. 25, No. 2, 1988, pp. 121–127.

[22]Eversman, W., and Tewari, A., "Consistent Rational-Function Approximation for Unsteady Aerodynamics," *Journal of Aircraft*, Vol. 28, No. 9, 1991, pp. 545–552.

[23]Eversman, W., and Tewari, A., "Modified Exponential Series Approximation for the Theodorsen Function," *Journal of Aircraft*, Vol. 28, No. 9, 1991, pp. 553–557.

[24]Dunn, H. J., "An Analytical Technique for Approximating Unsteady Aerodynamics in the Time Domain," NASA TP 1738, Nov. 1980.

[25]Parker, R., "Resonance Effects in Wake Shedding From Parallel Plates: Calculation of Resonant Frequencies," *Journal of Sound and Vibration*, Vol. 5, No. 2, 1967, pp. 330–343.

[26]Mahajan, A. J., Bakhle, M. A., and Dowell, E. H., "An Efficient Procedure for Cascade Aeroelastic Stability Determination Using Nonlinear, Time-Marching Aerodynamic Solvers," AIAA Paper 93-1631-CP, April 1993.

[27]Hall, K. C., Florea, R., and Lanzkron, P. J., "A Reduced Order Model of Unsteady Flows in Turbomachinery," American Society of Mechanical Engineers, ASME Paper 94-GT-291, June 1994.

[28]Whitehead, D. S., "Classical Two-Dimensional Methods," *AGARD Manual on Aeroelasticity in Axial Flow Turbomachines. Vol. 1: Unsteady Turbomachinery Aerodynamics*, edited by M. F. Platzer and F. O. Carta, AGARD, Neuilly-sur-Seine, France, AGARD-AG-298 Vol. 1, March 1987, Chap. 3.

[29]Bisplinghoff, R. L., Ashley, H., and Halfman, R. L., *Aeroelasticity*, Addison-Wesley, Reading, MA, 1955, pp. 281–286.

[30]Smith, B. T., Boyle, J. M., Dongarra, J. J., Garbow, B. S., Ikebe, Y., Klema, V. C., and Moler, C. B. *Matrix Eigensystem Routines—EISPACK Guide*, 2nd ed., Vol. 6 Lecture Notes in Computer Science, Springer-Verlag, New York, 1976.

[31]Humar, J. L., *Dynamics of Structures*, Prentice Hall, Englewood Cliffs, NJ, 1990, pp. 567–572.

[32]Theodorsen, T., "General Theory of Aerodynamic Instability and the Mechanism of Flutter," NACA Rept. 496, 1935.

[33]Desmarais, R. N., "A Continued Fraction Representation for Theodorsen's Circulation Function," NASA TM-81838, Sept. 1980.